The influence of additive manufacturing on the micromilling machinability of Ti6Al4V: A comparison of SLM and commercial workpieces

Fábio de Oliveira Campos, Anna Carla Araujo, André Luiz Jardini Munhoz, Shiv Gopal Kapoor

The influence of additive manufacturing on the micromilling machinability of Ti6Al4V: a comparison of SLM and commercial workpieces

Abstract

Ti6Al4V produced by selective laser melting (SLM) is replacing the use of casting workpieces as it is a net-near shape process that can maintain its mechanical and biocompatibility properties and it can produce scaffolds geometry reducing the workpiece weight. Typically, the microstructure produced by SLM differs from casted workpieces, the surface roughness of SLM is also different is also higher compared to casted pieces. If it is needed precision and smooth surfaces, it is necessary to add machining after SLM, especially for the production of channels smaller then 1 mm, which is the case of micromilling. For the definition of micromilling, it is not recommended to use the ones indicated for meso scale and there are few studies on the micromilling of Ti6AL4V implants produced by SLM. This study compares the machinability of the standard commercial Ti6Al4V with produced by SLM during micromilling process using different feed per tooth configurations (from 0.5 to 4.0 μm). The analysis of machinability considered cutting forces, surface roughness, burr formation analysis and microchips morphology. Despite presenting higher strength and hardness, SLM material presented higher machinability with lower forces, lower surface roughness and less burs, explained by the SLM microstructural of fined acicular α' martensite due to the rapid cooling of the material.

Keywords: Micromilling, Titanium Alloys, Additive Manufacturing, Selective laser melting

1. Introduction

Titanium alloy Ti6Al4V is the most used titanium-based material to manufacture biomedical implants. It presents good mechanical strength and hardness while preserves the key titanium properties for implants application, such as good corrosion resistance and biocompatibility (Mjöberg et al., 1997). Despite some studies that implants made by Ti6Al4V may not be good for a long time (Zaffe et al., 2004; Mittal et al., 2018), it has generally been a good candidate for biomedical applications since other common materials, including CP-Ti, do not possess the necessary strength.

Additive manufacturing (AM) processes have been recently studied in order to produce biomedical implants and one of the most suited AM process to manufacture implants is selective laser melting (SLM). Selective laser melting is a powder-based AM process, which consists basically of solidifying metallic powder layers, previously defined by slicing a three dimensional model of the desired part, on top of each other until the part is completely fabricated (Kruth et al., 2007). One of the main advantages of SLM is that it is one of the few additive manufacturing operations that produces fully dense parts.

In addition, SLM allows the fabrication of implants with different porosity rates which can result in different values of elastic modulus. The elastic modulus of an implant is related to the stress shielding phenomenon, which

is the loss of bone density around the implant due to a high difference between the elastic modulus of the implant and of the bone. Also, it is well known that rough surfaces can promote better and faster bone apposition, being more osteoconductive than a smooth surface. Selective laser melting makes it possible to achieve different surface roughness by modifying the three dimensional model. Moreover, a finishing manufacturing process such as micromilling can be used to produce details on the SLM produced part. Micromilling can be applied to achieve surface roughness that can not be achieved by SLM, to change the surface of parts manufactured by SLM with the objective to increase osteointegration or even change implant wettability.

There are several studies that cover the properties of titanium parts manufactured by SLM process (Pattanayak et al., 2011; Traini et al., 2008). Titanium workpieces produced by SLM present fined grain microstructure which leads to higher mechanical resistance and hardness. In general, SLM produces materials with different mechanical and micro structural properties which will highly affect machining operations. However, only a few papers have been published covering how the mechanical and micro structural properties imposed by SLM process into the workpiece will affect its machinability. Hojati et al. (2020) studied the differences between micromilling titanium alloy produced by Electron Beam Melting, which is an AM process that results in a similar material to SLM, and conventional titanium. They analyzed cutting force, surface roughness and burr formation with different feeds per tooth. They found that EBM titanium presented the same or lower forces although it presented higher hardness. Bonaiti et al. (2017) investigated the micromilling machinability of Ti6Al4V produced by additive manufacturing, analyzing cutting forces, roughness and burr formation. They found several differences when comparing the AM material with the standard titanium alloy: AM material presented higher hardness due to a finer microstructure; standard titanium presented higher surface roughness than AM titanium; despite presenting increased hardness, AM titanium presented lower cutting forces; and standard titanium presented better results considering burr formation. However, in their study, the workpieces had a high porosity level. Polishetty et al. (2017) studied the differences between standard Ti6Al4V and the same material produced by selective laser melting in turning, considering cutting forces and surface roughness. They found out that the cutting forces were higher for the SLM material due to increased strength presented by the material. Thus, SLM material presented lower surface roughness because of their increased hardness and brittleness.

This paper aims to perform a comprehensive micromilling machinability analysis comparing standard Ti6Al4V and Ti6Al4V produced by SLM regarding cutting forces, specific cutting forces, surface roughness, top burr height and chips morphology. Micromilling and its mechanism are described first. It is followed with the development of experimental work and discussion of machinability of both materials.

2. Micromilling cutting mechanism

Despite presenting several similarities regarding the conventional macro milling operation, micromilling process has some fundamental differences which make it a more complex process. While presenting basically the same kinematics and same general characteristics, the miniaturization of the milling process leads to the size effect phenomenon which considerably affects the cutting mechanic and, as a consequence, the expected machining results (Vollertsen et al., 2009).

The conventional cutting mechanics in macromilling usually considers the cutting edge of the tool as perfectly sharp. There is almost none contact between the machined surface and the flank surface of the tool and the chip is removed by shearing stress due to the interaction between the sharp edge and the material. The undeformed chip thickness, t_c, is significantly higher than the cutting edge radius r_β. However, in micromilling, cutting edge radius dimension is often of similar dimension to the uncut chip thickness, it is a function of other parameters $t_c = f(f_t, \phi, z, r_\epsilon)$.

This change of the cutting mechanics leads to the appearance of the minimum chip thickness t_{cm}, below which there would be no actual material cutting, but only plastic deformation of the material followed by elastic recovery, phenomenon called ploughing. Chae et al. (2006) proposed a basic cutting mechanism based on the relation between the chip thickness and minimum chip thickness which works as follows:

(a) $t_c > t_{cm}$ - material removal will occur mainly by shearing. Ploughing can usually also be observed due to the elastic recovery of the material;

(b) $t_c \approx t_{cm}$ - ploughing phenomenon occurs, but shearing also has a role in chip removal. Here, a volume of the material is removed by shearing while the other part is plastically deformed;

(c) $t_c < t_{cm}$ - ploughing is dominant and almost the entire material volume is only plastically deformed followed by elastic recovery. Bao and Tansel (Bao & Tansel, 2000) developed an alternative equation for computing chip thickness during micromilling taking into consideration the cutting tool radius r_ϵ.

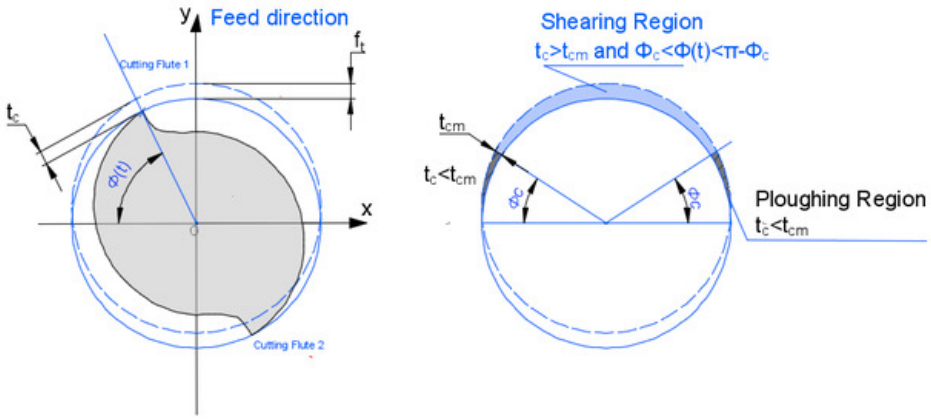

Figure 1: Ploughing and shearing regions in full immersion micromilling.

Due to this new approach in cutting mechanics for micromilling, machining results can be significantly different from expected. For example, when working in ploughing region, tool wear can rapidly increase affecting surface roughness and cutting forces. Also, as seen in Fig. 1, in full immersion milling, cutting tool might work under ploughing for specific flute positions which can influence burr formation as the material would not be cut, but only deformed.

Size effect can also affect machining results for materials with more than one microstructural phase. Materials which are usually considered to have a homogeneous microstructure might need to be studied as presenting heterogeneous microstructure. As the undeformed chip thickness and cutting edge radius are reduced, depending on

the grain size of the material, it can be around the same dimension of the chip thickness, meaning that the tool flute can engage each time in a different microstructure phase or grain which might present different mechanical properties (Mougo et al., 2018).

3. Material characterization

This study deals with two different materials: commercial Ti6Al4V alloy and Ti6Al4V produced by SLM. *Biofabris - Instituto Nacional de Ciência & Tecnologia em Biofabricação* (National Institute of Science and Technology in Biomanufacturing) produced the SLM Ti6Al4V workpiece in the laser sintering system EOS M270. The Ti6Al4V powder has the morphology shown in Fig. 2a. The particles have a spherical shape with different diameters.

The process parameters used for manufacturing in SLM equipment were: the laser power was $170W$, scanning speed was 1250 mm/s (75 $\mu m/min$), layer thickness is 30 μm and hatch space 0.1 mm. They were specified so that a fully dense Ti6Al4V workpiece was obtained as presented in Fig. 2b. The sample suffered a stress relief process to reduce residual stresses and avoid warpage.

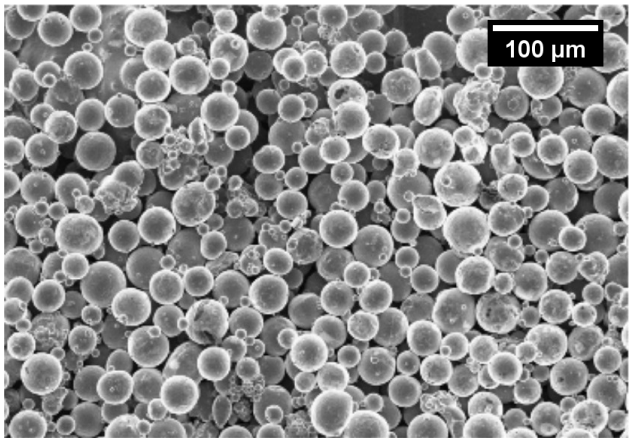

(a) Ti6Al4V powder morphology.

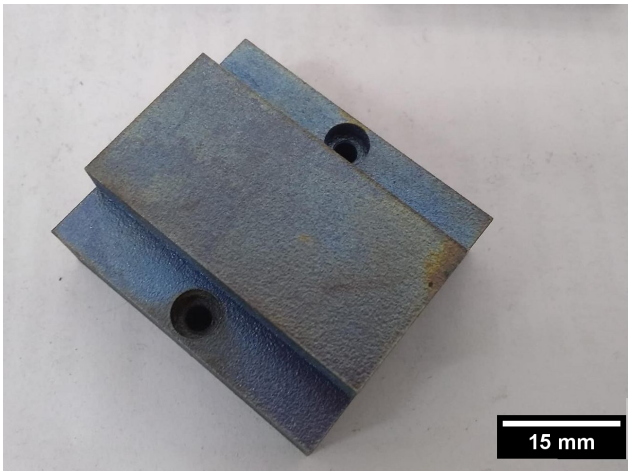

(b) SLM workpiece.

Figure 2: SLM workpiece.

The microstructure and mechanical properties of both materials were analyzed as they are directly related to the behavior of the materials during machining. This section details the procedure for the characterization of the materials and for the micromilling experiments as well as the equipment and tools used.

3.1. Materials microstructure

The microstructure of both materials was analyzed under an optical microscope. The preparation of the workpieces was made through polishing and Kroll's reagent was used for chemical attack. The microstructure of standard Ti6Al4V alloy is presented in Fig. 3a and is composed by equiaxed alpha grains with alpha-beta intergranular phase. The alpha grains size varied from 10-20 μm and it is similar to literature results (Motyka et al., 2012). The microstructure of SLM sample shows shows an acicular α' martensitic microstructure (Fig. 3b). The acicular martensite grains presented width dimensions ranging between 1 and 2 μm. This phase is a consequence of beta

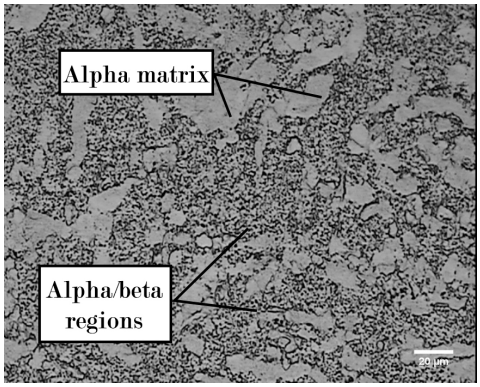

(a) Commercial alloy microstructure.

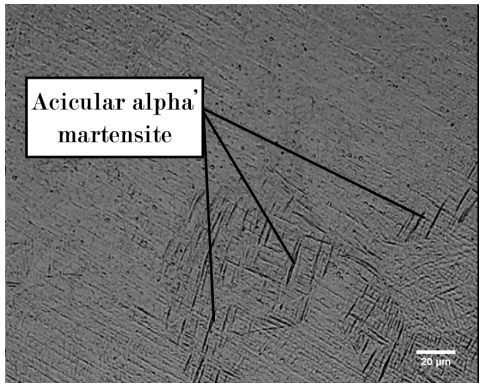

(b) SLM alloy microstructure.

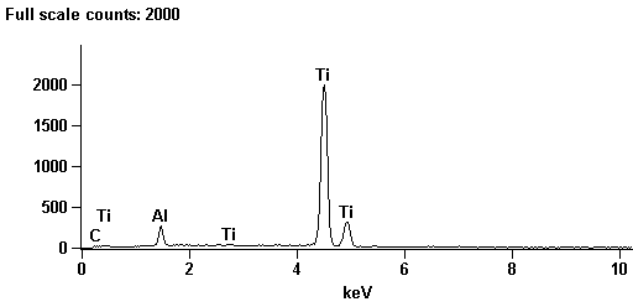

(c) Commercial alloy EDS result.

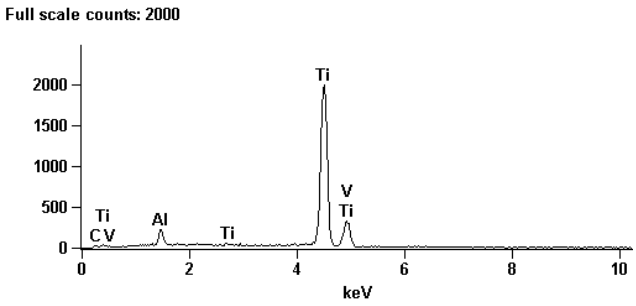

(d) SLM alloy EDS result.

Figure 3: Microstructure and Energy Dispersive X-ray Spectroscopy results.

transformation and it is achieved through quenching. As it can be seen, the microstructure presents refined grains in comparison with Ti6Al4V standard annealed alloy. The microstructure showed no sign of voids, indicating that a fully dense material was achieved. A porosity test was made to measure the percentage of density of the SLM sample, using the Archimedes method, and a porosity of 1.7% was measured for the SLM sample.

Energy dispersive X-ray spectroscopy (EDS) analysis identified only the standard composition as expected in both cases. The results are presented in Fig. 3c and Fig. 3d. For the alloy sample, the energy peak related to the presence of vanadium ($K\alpha_1$) is masked by the $K\beta_1$ titanium peak as they overlap. The SLM sample presented a major peak for titanium presence and secondary peaks for aluminum and vanadium.

3.2. Mechanical properties

Two mechanical tests were carried out: hardness (in SLM and commercial titanium) and bending flexural (in SLM) test. Vickers hardness tests were carried out in both materials with loads of 30 kgf for cycles of 20 s using an Indentec universal tester. Five measurements of hardness were taken for each sample in different random positions after proper surface preparation using the procedure described in ASTM E92-17. As the microstructure of both materials, SLM and commercial titanium alloy, were regularly distributed through all the analyzed surface, no specific locations were specified for the measurements. Three points flexure tests were performed in the SLM sample and the flexural modulus and flexural strength of the materials were computed. It was used samples with dimensions of 10 x 4 x 2 mm. The flexural properties of the alloy sample are taken from the literature (Campos et al., 2019).

Table 1 summarizes the mechanical properties results and includes the cortical bone properties obtained from the literature. The differences between the materials can be explained by their microstructure. Titanium alloy flexural strength presented more than twice the value when fabricated by SLM, but also presented a decrease in stiffness with the flexural modulus reducing from 114 to 19 GPa. Analyzing their microstructure, it is clear that a strong grain refinement process occurred that led the strength increase, due to the higher presence of grain boundaries and the difficulty for the dislocations motion. Reduced stiffness is a good material improvement considering the biomedical implants application. The flexural modulus of bone can vary between 7 and 30 GPa. The stiffness presented by the SLM material is closer to the human bone value which can overcome the stress shielding phenomenon (Campos, 2018).

Table 1: Summarized mechanical properties and literature data (*) for flexural strength and modulus and hardness.

Property	**Ti6Al4V**	**SLM**	**Cortical Bone**
Flexural strength (MPa)	900 (*)	2011	195 (*)
Flexural modulus (GPa)	114 (*)	19	30 (*)
Hardness (HV30)	318	370	-

The Vickers hardness tests results followed the flexural strength behavior. Selective laser melting sample presented a higher value (369 HV30) than the standard titanium alloy (318 HV30). It is important to point out that in selective laser melting, the workpiece is built layer by layer in a pre-determined direction which can lead to anisotropic behavior regarding directions normal and parallel to the building direction. Hardness was measured normal to the building direction which is where the experiments would be performed on.

4. Micromilling experiments

The micromilling experiments were performed on a CNC Mini-Mill/GX from Minitech Machinery using 500 μm uncoated carbide square-end-mills with 2 flutes (Mitsubishi Materials - MS2SSD0050). The microtools were analyzed under a Zeiss scanning electron microscope, model DSM 940. The measurements yielded the cutting edge radius r_β of 2-2.5 μm, corner radius of 10 μm and helix angle of 26° as can be seen in Fig. 4.

For force measurements, it was used the Kistler dynamometer MiniDyn 9256C2, the Kistler charge amplifier 5070A10100 and the data acquisition board USB 6251 from National Instruments. Figure 5 shows the axis configuration of force measurements in relation to the workpiece.

The resultant force was calculated using the three orthogonal measured components from the dynamometer. For each tool revolution, the curve achieves a maximum resultant force value when chip load is maximum. The results presented in this article are the average value of the maximum resultant force in 40 tool revolutions for each experiment. The micromilling dynamometer was sensible to the desired bandwidth and spindle speed frequency was 300 Hz and the tooth passing frequency was 600 Hz. A band-pass filter was performed in order to dismiss unwanted cutting force signal frequencies.

For surface roughness and top burr height measurements, a profilometer Form Talysurf Intra120 with stylus 112/2009, and 2 μm corner radius was used. Three roughness measurements were performed along the feed direction

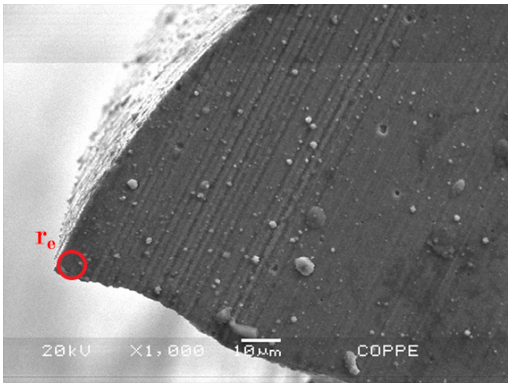

(a) Cutting edge radius - r_β

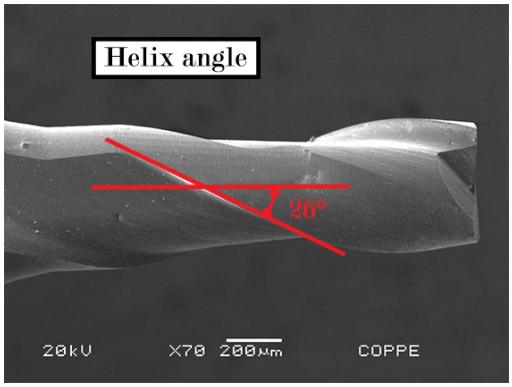

(b) Helix angle - λ

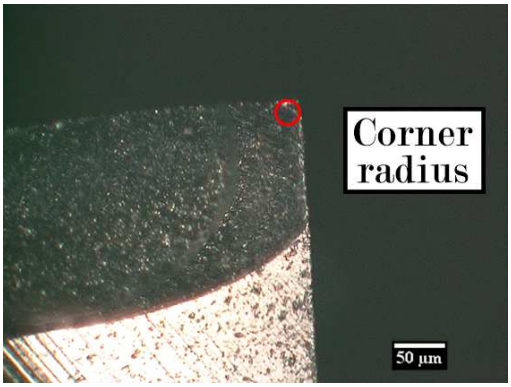

(c) Corner radius - r_ϵ

Figure 4: Microtool geometry.

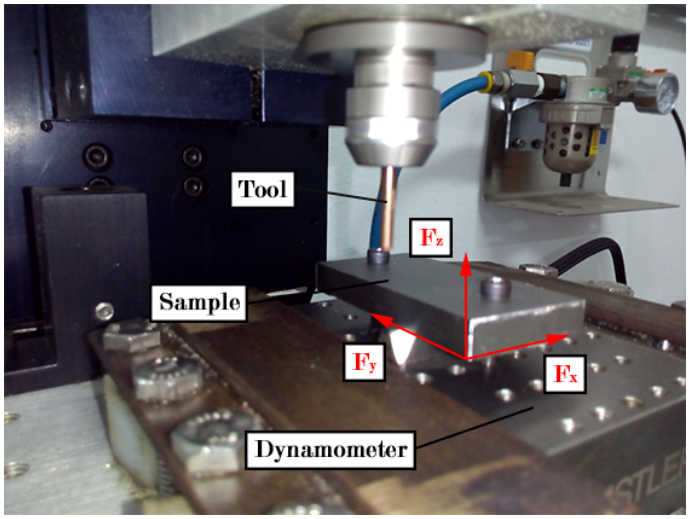

Figure 5: Force measurement setup.

on the bottom surface of each machined groove as showed in Fig. 6a. Cut-off filter used was 0.08, according to ISO 4288-1996, and it was specified considering the feed per tooth used in the micromilling experiments.

Top burr height measurement was performed by taking the profile of each groove as showed in Fig. 6b. The procedure was developed in order to compare the burrs produced by micromilling both materials. Also, five

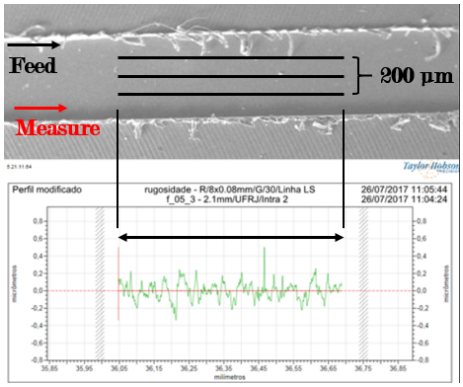

(a) Surface roughness.

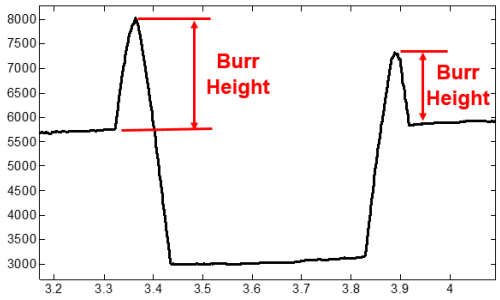

(b) Procedure to measure and compare burr height.

Figure 6: Surface roughness and burr measurement details.

measurements were taken in different positions along the grooves in order to be representative. This methodology allowed correlation between relative values and the SEM images. Chips were collected in all experiments and for the chips morphology and grooves surface analysis, SEM and USB AM3715TB Dino-Lite Edge hand-held digital microscope images were used.

The workpieces were flattened to provide regular axial depth of cut variation. The surface preparation used 3 mm diameter milling tool, cutting speed was 37.7 m/min (4000 rpm), feed rate was 120 m/min (feed per tooth of 0.015 mm) and axial depth of cut was 30 μm.

4.1. Design of experiments

Considering the cutting edge radius value (r_β = 2.0-2.5 μm), feed per tooth range for the micromilling experiments is specified so it would be possible to clearly identify both ploughing and shearing regions. The cutting speed, axial depth of cut and cutting length are kept constant during machining. Full immersion machining was chosen so that the tool would engage in both up and down milling. The cutting parameters are shown in Tab. 2.

Table 2: Cutting data.

Parameter	**Value**
Tool diameter	500 μm
Spindle speed	18000 rpm
Cutting speed	28.3 m/min
Feed per tooth	0.5 - 4.0 μm
Axial depth of cut	40 μm
Radial depth of cut	500 μm
Cutting length	4 mm
Cutting system	Dry cutting

At first, the procedure described in standard NF E66-520 is used, where an optimal feed per tooth is found by analyzing specific cutting energy results. In this procedure, f_t is defined by increasing values, in this case from

0.5 to 4 μm. In order to study the tool wear influence on the measured outputs, a second batch of experiments is performed decreasing feed per tooth after each test. The first batch, with increasing feed, is the batch A and the second one, with decreasing feed, is the batch B as shown in Tab. 3.

Table 3: Design of experiments.

Experiment	**Batch**	**Feed (μm/tooth)**	**Machined length**
1 to 8	A	0.5 up to 4.0	4 mm in each feed per tooth (total of 32 mm)
9 to 16	B	4.0 down to 0.5	4 mm in each feed per tooth (total of 32 mm)

5. Experimental results and discussion

This section presents the experimental results and discussion of the micromilling experiments regarding cutting force, surface roughness, top burr and chips morphology analysis for both materials, including commercial titanium alloy and SLM produced titanium alloy.

5.1. Cutting forces and specific cutting energies

Figure 7a presents the maximum force results for the commercial titanium alloy and the SLM alloy for batch A (increasing feed) and batch B (decreasing feed) and the error bars represent +/- 1.96σ. The general force behavior corresponds to the expected result: experimental cutting force increases when increasing feed per tooth as the cutting area is linearly proportional to f_t.

If there was no tool wear, the points for both batches should be overlapped which, in general, did not happen. As expected, tool wear played a great role during the experiments. Since tool wear had such an important impact, the corresponding experiments of each batch can not be considered replicas and it would not be correct to compute the force average. Therefore, each batch was analyzed separately.

The force curve trend for batch B did not show a wide angular coefficient as batch A which is another indication of tool wear. This is because when decreasing feed per tooth, the cutting force should be smaller. Tool wear ends evening up the feed per tooth effect on the cutting force.

Comparing the results between the materials, the experimental resultant force showed in general an inverse trend from what was expected, considering the hardness of test samples. It is expected that SLM should present higher forces as it has significantly higher strength and hardness, but it presented lower cutting forces. This result is in compliance with other studies in micromilling of titanium alloys where cutting forces were found smaller for higher hardness material. Bonaiti *et al.* (Bonaiti et al., 2017), for example, found lower cutting forces when milling additive manufacturing Ti6Al4V with different porosities using a 500 μm tool and different feed per tooth in comparison with commercial Ti6Al4V. Hojati *et al.* (Hojati et al., 2020) also found lower forces when micromilling a fully dense additive manufacturing titanium in comparison to conventional extruded titanium, even though it presented higher hardness.

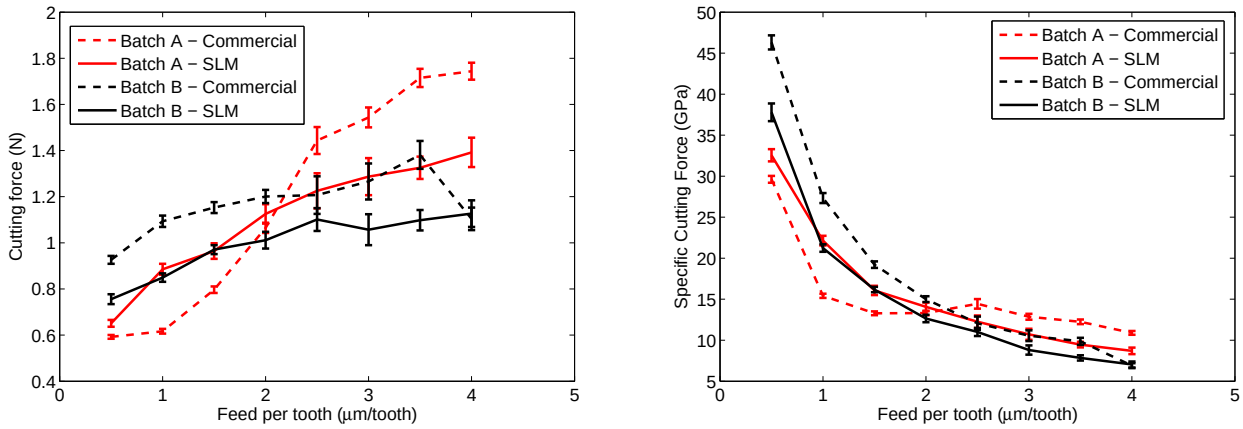

(a) Cutting force results for Ti6Al4V alloy and SLM produced titanium alloy.

(b) Specific cutting force results for Ti6Al4V alloy and SLM produced titanium alloy.

Figure 7: Experimental force results.

There are several possible reasons that could help in explaining the behavior. In micromilling, the microstructure of the material can play an important role, specially in machining forces. Despite the differences in grain size, commercial alloy and SLM alloy presented different phases and grains shape. While the commercial alloy presented near equiaxed alpha grains with alpha/beta regions in between, SLM sample presented acicular alpha‘ martensite in alpha matrix. Abbasi *et al.* (Abbasi et al., 2016) studied the influence of the microstructure on the machinability of the titanium alloy, applying different heat treatment to the material. They concluded that machinability can be positively affected by an improved microstructure constituents.

Besides the microstructure, tool wear can have influence on the cutting force during the experiments. Analyzing batch A, the force relation between the materials changes in the middle of the experiments. As this fact did not occur for batch B, it can mean that when the tool was new, forces for SLM were higher, but as the tool for commercial alloy worn more than for the SLM alloy, the cutting force for the commercial alloy became higher. For batch B, the forces for SLM material were higher in all feeds because as it started with a high feed per tooth, the difference in tool wear might have been significant from the first experiment.

Using the maximum resultant forces, specific force was computed and is shown in Fig. 7b. Both materials presented the same general behavior: a decrease in the value while feed per tooth is increased. Both A and B batches show a change from an almost linear behavior to a non-linear behavior when feed decreases. As feed value is decreased, specific cutting force tends to quickly increase, while increasing the feed it tends to approximate to a constant level. This is an indicative of ploughing phenomenon becoming more present as feed per tooth decreases.

Examining the figure, it can be seen that for both materials for a feed of 0.5 μm/tooth, both A batches presented a higher value for the specific force than for B batches, while for 4.0 μm/tooth, the opposite occurred. This is an indication of the tool wear role in the specific cutting force values. The specific force can be understood as the force needed for the tool to cut a chip with 1 mm^2 area. Therefore, it is influenced by many factors, including the tool geometry. When the tool wears, the cutting edge radius and point radius change, affecting the force needed to cut the material.

5.2. Surface roughness

In conventional milling surface roughness, in general, increases when feed per tooth is raised due to geometric relations considering, among other parameters, the feed per tooth and the corner radius of the tool. However, in micromilling, several results show that roughness can present a different behavior when varying feed per tooth. Surface roughness results are shown in Fig. 8. The error bars represent +/- 1.96σ.

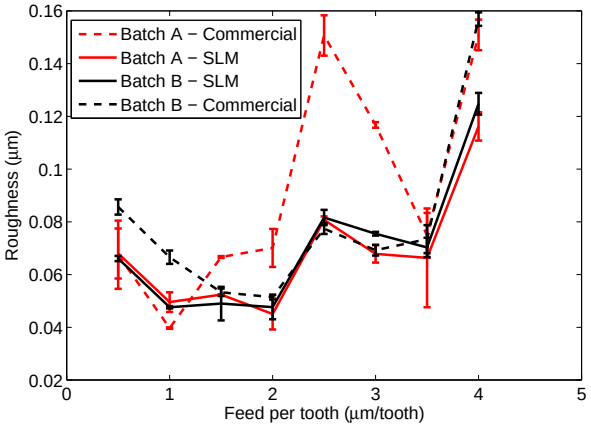

Figure 8: Surface roughness results for Ti6Al4V alloy.

It can be seen that the surface roughness behavior when increasing feed per tooth does not follow the conventional milling standard results. It presents different tendencies according to the feed window that it is analyzed for. It is possible to roughly specified three different regions in the roughness behavior according to feed per tooth.

The first region is characterized by a decrease in roughness values when increasing feed from 0.5 to more or less 1.5 μm/tooth. This can be explained by the ploughing phenomenon which can be dominant in this window of feed and cause an uneven plastic flow of material that can prejudice surface finishing. The second region, when feed per tooth is increased from 1.5 to 3.5 μm/tooth, shows an unstable behavior, initially increasing and then decreasing or staying more or less at the same level. In this region, the cutting edge radius value of the microtool is similar to the feed per tooth and it can be a possible reason for the instability of the roughness results. The third part, which is related to the increase of feed from 3.5 to 4 μm/tooth represents a strong rise in the roughness values. This feed window represents the same trend expected for conventional milling and it shows that in this range, feed per tooth is high enough to have shearing dominant.

For the SLM sample, it is noticed that tool wear did not present as much influence as it presented for the alloy sample. Despite the fact that several corresponding points did not overlap, both batches presented similar trend. Also, the roughness differences between the corresponding points were not so large. Surface integrity is deeply connected to the corner radius value and shape. Depending on how the tool wear is affecting the tool shape, it can sometimes favor or prejudice surface roughness. The rapid growth of roughness values from 2 to 2.5 μm/tooth for the commercial sample and the later return to normal values can be a consequence of this wear mechanism.

Comparing the materials, considering each batch, SLM sample presented a better surface roughness result in general which can be explained by the lower ductility and higher hardness that SLM titanium presented leading to less plastic flow during cutting.

5.3. Burr height results

Burr measurement can present expressive variations as there is not a standard procedure for measurement and it can be influenced by several factors. Because of this, burr formation analysis took into consideration both top burr height measurements and visual examination.

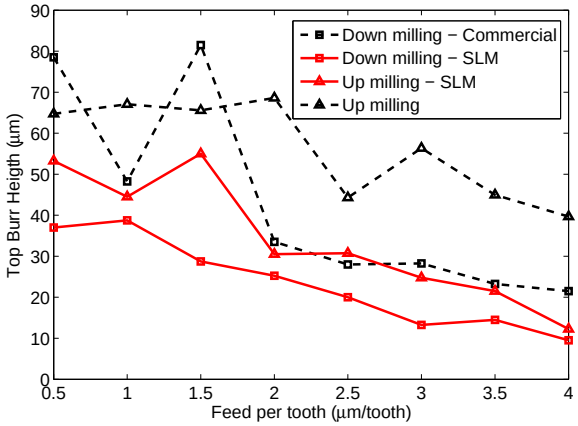

Figure 9: Top burr height measurement results for Ti6Al4V.

Figure 9 shows top burr measurement results for both materials. A general burr formation trend can be identified when varying feed per tooth: it decreases when increasing feed. Although for small feed values this trend is not identifiable, after 2.0 μm/tooth, it becomes evident. As feed per tooth gets closer to the cutting edge radius, shearing of the material starts to be replaced by ploughing mechanism where the material is plastically deformed more than cut off.

The top image from the grooves machined with feeds of 1.0 and 3.5 μm/tooth is shown in Fig. 10 and it confirms the previous analysis. It can be seen that burr formation for 3.5 μm/tooth was clearly smaller than for 1.0 μm/tooth. Besides, in general, up milling presented less burr formation or smaller burrs than down milling.

Comparing the commercial sample with the SLM alloy, the SLM presented a better result having less burrs. In addition, in spite of presenting less tool wear, the SLM sample also has a more brittle behavior as compared to Ti alloy, which should also contribute to the smaller burr values. The chips tend to break and be removed easily and do not stay connected to the workpiece.

5.4. Chips morphology

Microchips generated during the experiments for 0.5 and 4.0 μm/tooth are shown in Fig. 11. For both materials, it can be seen that the chip length decreases when increasing feed per tooth varying from a length of around 0.5 mm for 0.5 μm feed per tooth to around 200 μm for 4 μm/tooth for the alloy sample and of more than 2 mm to around 250 μm for for SLM alloy. Analyzing the entire feed range, it is noticed that feeds higher than 2.0 μm/tooth clearly shows smaller length.

It is important to notice that for the SLM material, small feeds lead to longer chips higher than the theoretical tool engagement with the workpiece. This can happen when ploughing phenomenon is dominant. As material

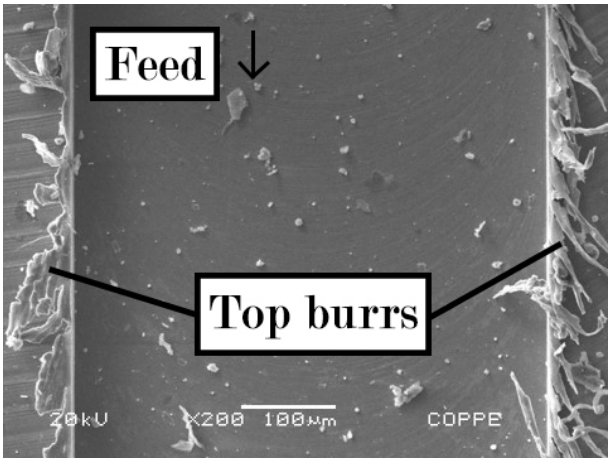

(a) Titanium alloy - $f_t = 1.0$ μm/tooth.

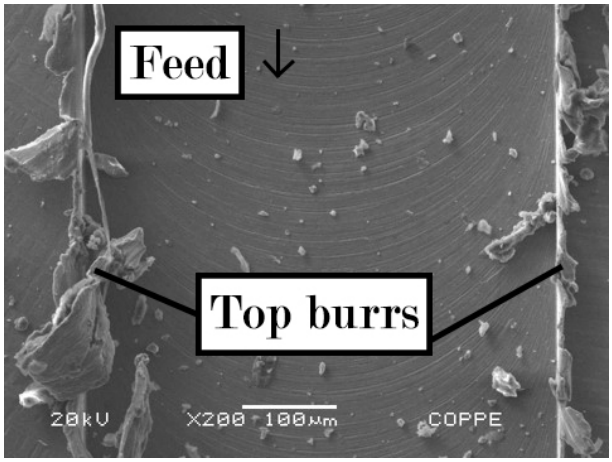

(b) Titanium alloy - $f_t = 3.5$ μm/tooth.

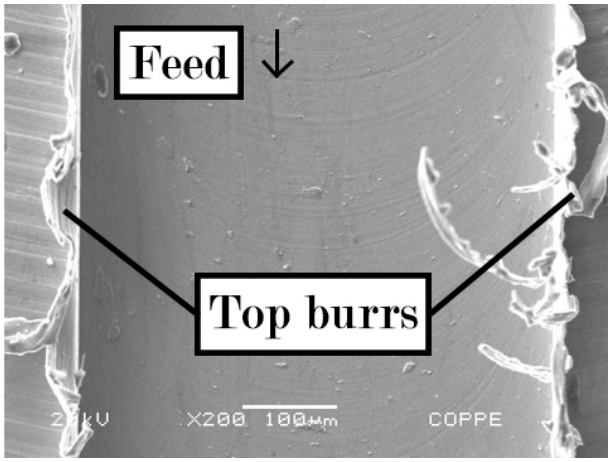

(c) SLM alloy - $f_t = 1.0$ μm/tooth.

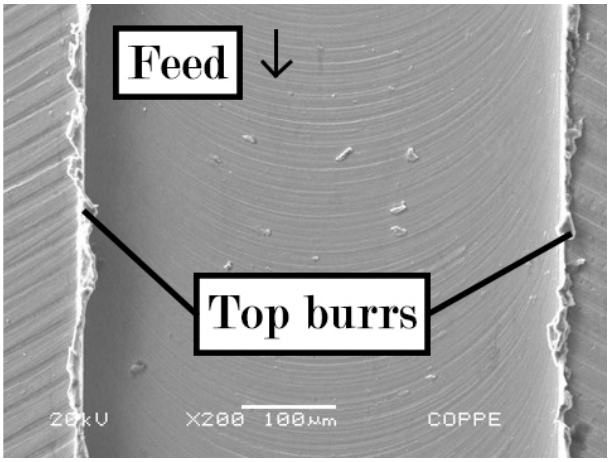

(d) SLM alloy - $f_t = 3.5$ μm/tooth.

Figure 10: Grooves and top burrs SEM images. Upmilling: right; Downmilling: left.

removal can sometimes not happen, a flute can remove the material left by the previous flute engagement leading to higher chip length.

6. Conclusions

This study dealt with two different titanium-based materials: commercial Ti6Al4V alloy and Ti6Al4V fabricated by SLM. The micromilling machinability of each material considering cutting forces, surface roughness, burr formation, microchips morphology as well as their mechanical properties and the influence on each parameter were compared and analyzed. Specific conclusions done for this study are:

- Microstructure analysis of both materials were also conducted. The SLM sample presented fined acicular alpha' martensite in alpha matrix. Selective laser melting sample presented an increase of strength and hardness regarding their standard related materials as well as a decrease in the stiffness and a more prominent brittle behavior;

(a) Titanium alloy - $f_t = 0.5$ μm/tooth.

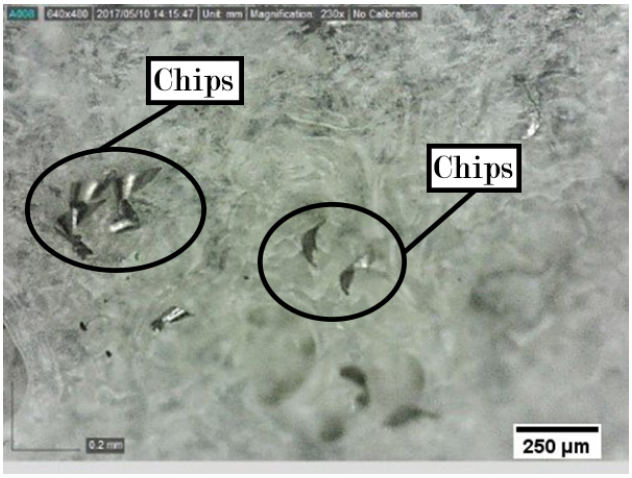

(b) Titanium alloy - $f_t = 4.0$ μm/tooth.

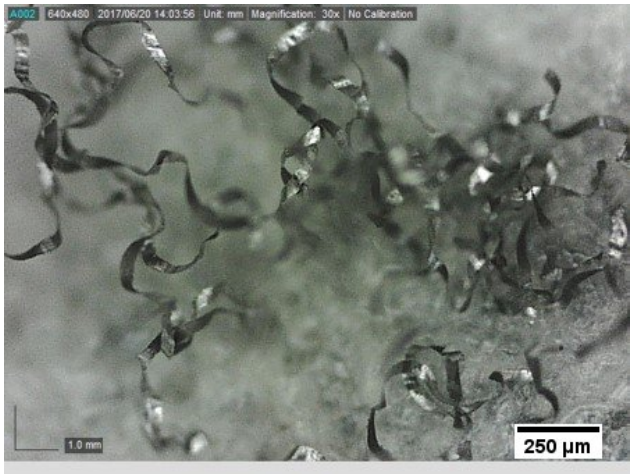

(c) SLM alloy - $f_t = 0.5$ μm/tooth.

(d) SLM alloy - $f_t = 4.0$ μm/tooth.

Figure 11: Optical images of chips collected during micromilling experiments of Ti6Al4V and SLM titanium alloy.

- The SLM sample presented lower cutting and specific force values than the commercial alloy, despite presenting higher strength and hardness. Hardness of the SLM material was 16% higher, but forces for this material was in average 9.3% lower. This result can be related to its finer microstructure as well as to the fact that the tool was less affected by tool wear. This result is in conformity with other studies (Bonaiti et al., 2017; Hojati et al., 2020; Abbasi et al., 2016);

- Roughness behavior when varying feed per tooth was similar for both materials, presenting variations at feeds per tooth close to the ploughing-shearing transition and to the tool cutting edge radius. In general, SLM sample presented better surface roughness results for almost all feeds per tooth studied. his is probably related also to the lower tool wear in comparison with the other material as well as the brittle characterictics the material presented leading to less plastic flow during cutting;

- Burr formation during down milling was higher than in up milling for both materials as well as a trend of decreasing burr formation when increasing feed per tooth was identified. Hence, when machining these

materials, it is suggested to plan the milling operation for the tool to work only in down milling;

- Selective laser melting presented less burr formation than the commercial Ti alloy. This behavior can be explained by the smaller tool wear occurred during the process and affected less the cutting edge radius that is directly related to burr formation. Besides, it had a more brittle behavior than the Ti alloy which also might explain the less burr formation;

Overall, SLM Ti6Al4V presented higher machinability than commercial Ti6Al4V regarding its mechanical properties and the cutting force, roughness, burr formation and chips analysis.

References

Abbasi, S. A., Feng, P., Ma, Y., Zhang, J., Yu, D., & Wu, Z. (2016). Influence of microstructure and hardness on machinability of heat-treated titanium alloy Ti6Al4V in end milling with polycrystalline diamond tools. *Int J Adv Manuf Technol*, *86*, 1393–1405.

Bao, W., & Tansel, I. (2000). Modeling micro-end-milling operations. part i: analytical cutting force model. *International Journal of Machine Tools and Manufacture*, *40*, 2155 – 2173. URL: http://www.sciencedirect.com/science/article/pii/S0890695500000547. doi:https://doi.org/10.1016/S0890-6955(00)00054-7.

Bonaiti, G., Parenti, P., Annoni, M., & Kapoor, S. (2017). Micro-milling machinability of ded additive titanium Ti6Al4V. *Procedia Manufacturing*, *10*, 497 – 509. 45th SME North American Manufacturing Research Conference, NAMRC 45, LA, USA.

Campos, F. O. (2018). *Micromilling of titanium alloys: a comparison between workpieces produced by casting, ECAP and 3D printing (SLM)*. Ph.D. thesis Universidade Federal do Rio de Janeiro, Rio de Janeiro, Brazil.

Campos, F. O., Araujo, A. C., & Kapoor, S. G. (2019). Experimental Comparison of Micromilling Pure Titanium and Ti6Al4V. *Journal of Micro and Nano-Manufacturing*, *7*. URL: https://doi.org/10.1115/1.4043501. doi:10.1115/1.4043501.

Chae, J., Park, S., & Freiheit, T. (2006). Investigation of micro-cutting operations. *International Journal of Machine Tools and Manufacture*, *46*, 313 – 332. URL: http://www.sciencedirect.com/science/article/pii/S0890695505001306. doi:https://doi.org/10.1016/j.ijmachtools.2005.05.015.

Hojati, F., Daneshi, A., Soltani, B., Azarhoushang, B., & Biermann, D. (2020). Study on machinability of additively manufactured and conventional titanium alloys in micro-milling process. *Precision Engineering*, *62*, 1 – 9.

Kruth, J.-P., Levy, G., Klocke, F., & Childs, T. (2007). Consolidation phenomena in laser and powder-bed based layered manufacturing. {*CIRP*} *Annals - Manufacturing Technology*, *56*, 730 – 759.

Mittal, R. K., Singh, R. K., Kulkarni, S. S., Kumar, P., & Barshilia, H. (2018). Characterization of anti-abrasion and anti-friction coatings on micromachining response in high speed micromilling of Ti6Al4V. *Journal of Manufacturing Processes*, *34*, 303 – 312. URL: http://www.sciencedirect.com/science/article/pii/S1526612518307126. doi:https://doi.org/10.1016/j.jmapro.2018.06.021.

Mjöberg, B., Hellquist, E., Mallmin, H., & Lindh, U. (1997). Aluminum, alzheimer's disease and bone fragility. *Acta Orthopaedica Scandinavica*, *68*, 511–514.

Motyka, M., Kubiak, K., Sieniawski, J., & Ziaja, W. (2012). Hot plasticity of alpha beta alloys. In A. N. Amin (Ed.), *Titanium Alloys - Towards Achieving Enhanced Properties for Diversified Applications* chapter 5. Rijeka: InTech.

Mougo, A. L., de Oliveira Campos, F., & Araujo, A. C. (2018). Mechanistic study on micromilling of the super duplex stainless steel UNS S32750. *Journal of Manufacturing Processes*, *34*, 31 – 39. URL: http://www.sciencedirect.com/science/article/pii/S1526612518305310. doi:https://doi.org/10.1016/j.jmapro.2018.05.017.

Pattanayak, D. K., Fukuda, A., Matsushita, T., Takemoto, M., Fujibayashi, S., Sasaki, K., Nishida, N., Nakamura, T., & Kokubo, T. (2011). Bioactive ti metal analogous to human cancellous bone: Fabrication by selective laser melting and chemical treatments. *Acta Biomaterialia*, *7*, 1398 – 1406.

Polishetty, A., Shunmugavel, M., Goldberg, M., Littlefair, G., & Singh, R. K. (2017). Cutting force and surface finish analysis of machining additive manufactured titanium alloy Ti6Al4V. *Procedia Manufacturing*, *7*, 284 – 289. International Conference on Sustainable Materials Processing and Manufacturing, SMPM 2017, 23-25 January 2017, Kruger.

Traini, T., Mangano, C., Sammons, R., Mangano, F., Macchi, A., & Piattelli, A. (2008). Direct laser metal sintering as a new approach to fabrication of an isoelastic functionally graded material for manufacture of porous titanium dental implants. *Dental Materials*, *24*, 1525 – 1533.

Vollertsen, F., Biermann, D., Hansen, H., Jawahir, I., & Kuzman, K. (2009). Size effects in manufacturing of metallic components. *CIRP Annals*, *58*, 566 – 587. URL: http://www.sciencedirect.com/science/article/pii/S0007850609001693. doi:https://doi.org/10.1016/j.cirp.2009.09.002.

Zaffe, D., Bertoldi, C., & Consolo, U. (2004). Accumulation of aluminium in lamellar bone after implantation of titanium plates, ti–6al–4v screws, hydroxyapatite granules. *Biomaterials*, *25*, 3837 – 3844.